REVISTA CIENCIAS BIOMÉDICAS

ARTÍCULO ORIGINAL

Decellularization and in vitro characterization of porcine small intestine scaffolds for complex wound treatments

Descelularización y caracterización in vitro de matrices de intestino delgado porcino para el tratamiento de heridas complejas

Juan Pablo Ruiz[1], Sara Galvis-Escobar[1], María Antonia Rego[1], Juan David Molina[2], Catalina Pineda Molina[1]

[1] Biomedical Engineering Program, Engineering Faculty, Universidad CES, Medellín, Colombia.
[2] Veterinary Medicine Program, Veterinary Medicine, and Zootechnics Faculty, Universidad CES, Medellín, Colombia.

Para citaciones: Ruiz, J. P., Galvis Escobar, S., Rego, M. A., Molina, J. D., & Pineda Molina, C . (2023). Decellularization and in vitro characterization of porcine small intestine scaffolds for complex wound treatments. Revista Ciencias Biomédicas, 12(3), 102-120. https://doi.org/10.32997/10.32997/rcb-3023-4135

Recibido: 22 de marzo de 2023
Aprobado: 12 de junio de 2023

Autor de correspondencia:
Catalina Pineda Molina
cpinedam@ces.edu.co

Editor: Inés Benedetti. Universidad de Cartagena-Colombia.

ABSTRACT

Introduction: complicated skin injuries have become a global health problem, being difficult to treat due to the body's limited healing process. Many studies aim to enhance traditional treatments for skin injuries, which have many disadvantages. Therefore, wound healing research is aiming towards tissue engineering options, such as decellularized matrix, which have shown great healing and biocompatibility competencies.

Objectives: to obtain and characterize the properties of a decellularized biological matrix derived from the small intestine of animals.

Methods: porcine small intestine was prepared and decellularized using four different methods: Triton X-100, sodium dodecyl sulfate (SDS) and sodium deoxycholate (SDC) for one or two cycles of 6 hours or 24 hours, and peracetic acid for one cycle of 2 hours. The remaining DNA was quantified with Nanodrop and electrophoresis characterization. Histology stains and Scanning Electron Microscopy (SEM) were performed to assess surface structure and integrity. Resistance assays were conducted to measure mechanical strength. Finally, degradability assays with different buffers were performed.

Results: no differences between the decellularization protocols regarding remaining DNA were found, making protocols of one cycle of six hours more efficient. With the least remaining DNA content and better structure perseveration, TX-100 could be considered as the best protocol. No statistically difference between protocols and native tissue were found during the mechanical analysis. Biodegradability assays showed the expected degradability properties of the produced matrix.

Conclusions: promising results were achieved to obtain decellularized biological matrices that could serve as a treatment for complicated skin wounds. More in

vitro and molecular studies should be carried out in future studies to further characterize these scaffolds.

Keywords: Bioactive scaffold; decellularization; porcine small intestine; skin wound; tissue engineering.

RESUMEN

Introducción: las lesiones cutáneas complicadas se han convertido en un problema de salud mundial, siendo difíciles de tratar debido al limitado proceso de curación del cuerpo. Se han realizado estudios para mejorar los tratamientos tradicionales que tienen muchas desventajas. La investigación en cicatrización de heridas apunta a opciones con ingeniería de tejidos, como las matrices descelularizadas, con buenas propiedades de cicatrización y biocompatibilidad.

Objetivo: obtener y caracterizar las propiedades de una matriz biológica descelularizada derivada del intestino delgado de animales.

Métodos: el intestino delgado porcino se preparó y descelularizó utilizando cuatro métodos diferentes: Triton X-100 (TX-100), dodecil sulfato de sodio (SDS) y desoxicolato de sodio (SDC) para uno o dos ciclos de 6 horas o 24 horas, y ácido peracético para un ciclo de 2 horas. El ADN remanente se cuantificó con Nanodrop y electroforesis. Se realizaron tinciones histológicas y microscopía electrónica de barrido (SEM) para evaluar la estructura e integridad de la superficie. Se realizaron ensayos mecánicos para medir la resistencia de las matrices. Finalmente, se realizaron ensayos de degradabilidad con diferentes soluciones.

Resultados: no se encontraron diferencias entre los protocolos de descelularización con respecto al ADN remanente, siendo más eficientes los protocolos de un ciclo de seis horas. Con el menor contenido de ADN remanente y una mejor preservación de la estructura, TX-100 podría considerarse como el mejor protocolo. No se encontraron diferencias estadísticas entre los protocolos y el tejido nativo durante el análisis mecánico. Los ensayos de biodegradabilidad mostraron las propiedades de degradabilidad esperadas de la matriz producida.

Conclusión: se lograron resultados prometedores para obtener matrices biológicas descelularizadas que podrían servir como tratamiento para heridas cutáneas complicadas. Se deben realizar más estudios in vitro y moleculares a futuro para caracterizar aún más estas matrices.

Palabras Clave: Matriz bioactiva; descelularización; intestino delgado porcino; herida de piel; ingeniería de tejidos.

INTRODUCTION

Complex skin injuries such as open-wound, contaminated wounds, burns, and ulcers represent substantial economical, health and work-related burden in medical centers around the globe (1, 2). Just in the tropical region, one in every four hospitalizations are skin-related wounds, and 216 million dollars were spent towards wound care in 2017 alone (3).

These types of wounds are more prevalent in under and middle-developed countries due to high costs and resource scarcity, with the World Health Organization estimating that around 90% of skin injuries happen in these countries (2, 4, 5). Traditional treatments require a lot of effort and time, are costly, and usually include sustained uncomfortable and painful protocols, making them less than ideal for patient care (6).

The severity of skin pathologies and a need to find treatment alternatives for patients with skin conditions have become a priority in the fields of tissue engineering and regenerative medicine (7). To improve the current skin injury treatment landscape, tissue engineering aims to develop and implement biomaterials and novel biomedical devices capable of providing therapeutic effects and improved support, interacting with native tissue cells, and improving functional tissue repair (7).

The use of materials derived from extracellular matrix (ECM) from a variety of tissues, is of interest due to their capability of maintaining native properties and improving the effectiveness of the cellular interactions that contribute to the healing process (8). In particular, ECM-derived scaffolds, produced by decellularization of tissues, are of especial interest for clinical skin applications, given their content of collagen and other structural biomolecules, and the supplied tridimensional bioactive microenvironments for tissue repair and cell signaling (9). These scaffolds also provide important mechanical properties necessary to maintain functionality (10).

The present study provides an evaluation and comparison of the effectiveness of decellularization processes of porcine small intestine using different chemical solutions. Microstructural and mechanical properties were evaluated to compare the methods of decellularization of the samples.

METHODS

Tissue preparation and decellularization

Porcine small intestine was obtained from a cadaveric donor for reasons unrelated to the project contributed by Frigo Porcinos and frozen for preservation. Whole tissue was thawed and washed thoroughly with water, and sectioned in approximately 20 cm in length fragments, which were cut longitudinally to obtain sheet-like samples. The tissue's lumen was scraped to remove the mucosal layer using a plastic probe. No intestinal sections were excluded from the sample group: exclusion criteria included only sections with anatomical and physical affections (inflammation, changed vascularization, tears, apparent reduction of integrity and density). Samples were frozen at -80 °C until further use.

Porcine small intestine decellularization

Samples were immersed and washed with 1X PBS (for 1L of 10X PBS: 26.83 mM KCl, 14.70 mM KH_2PO_4, 1.37 mM NaCl, 84.53 mM Na_2HPO_4, appropriate amount of 1N NaOH or 1N HCl to adjust pH to 7.4) for four 30-minute cycles and one distilled water cycle under constant agitation at 300 rpm. Then, the specimens were immersed in aqueous solutions of the following chemical agents as previously suggested: Triton X-100 (0.5%) (11), sodium dodecyl sulfate (SDS) (0.1%) (12) or sodium deoxycholate (SDC) (4%) (13), during one or two cycles of 6-or-24-hours, or peracetic acid (0.1%) (14) one cycle of 2-hours, all under constant agitation at 300 rpm. After each decellularization cycle, washing protocol with PBS was repeated; samples were frozen and subsequently lyophilized for further use.

Quantification of nucleic acids

After decellularization and shredding of the scaffolds, 100 mg of lyophilized samples were digested using proteinase K at 50 °C from 24 to 72 hours under constant agitation at 80 RPM until complete homogenization, followed by

centrifugation at 2980 xg and 4 °C for 30 minutes to precipitate remaining proteins. The supernatant was purified with 2 ml phenol-chloroform-isoamyl and centrifuged at 4024 xg and 4 °C for 20 minutes. DNA was precipitated with 200 µl sodium acetate and 4 ml ethanol 100%, stored at -20 °C for 20 minutes and centrifuged following the previous parameters, and the pellet was resuspended in 4 ml ethanol 70% and centrifuged under the same conditions. The remaining ethanol was evaporated, and samples resuspended in 1 ml TE Buffer (10 mM Tris HCl (pH = 8), 1 mM EDTA) and stored at -20 °C until further use (14, 15).

Following DNA isolation, the DNA quantification was performed by spectrophotometry using a NanoDrop (Thermo Scientific 2000/2000C). The average of nucleic acid´s concentration was calculated from three replicates of each sample.

To determine the size of remaining DNA fragments, electrophoresis was performed in native and decellularized samples using a 1% agarose gel prepared with 1X TAE Running Buffer (for 1L of 50X TAE Running Buffer: 1.99 M Tris, 63.68 mM EDTA, 57.1 mL of glacial acetic acid) and stained using SYBR Green stain. A two-hour running time was established under constant voltage of 70 V (16). After completing the running, imaging was carried out using an ENDURO™ GDS Gel Documentation System, and the images were analyzed qualitatively comparing among replicate samples.

Histological analysis

Lyophilized samples were fixed by immersion in formalin 10% for 120 hours in a fume hood. Buffered samples were sent to the Clinica CES' pathology and histology laboratory, for hematoxylin and eosin staining. The stained samples were imaged under a microscope under 4X, 10X, 40X, and 100X magnifications for qualitative evaluation of the tridimensional structure to determine matrix integrity and collagen fiber organization (12). Sections were selected based on how representative they are of the integral tissue, and pictures were taken for each magnification using a Leica Microsystems ICC50 HD microscope-adapted camera.

Scanning Electron Microscopy

Scanning electron microscopy (SEM) was performed at the University Research Center at Universidad de Antioquia to obtain high-resolution images of native and decellularized matrix' surface to observe tissue integrity, topography, and porosity of the tissue. The lyophilized matrices were cut into 20 mm x 20 mm fragments and coated with gold to better capture the radiation emitted by the equipment and increase the resolution of the images obtained (17). This study was performed using a JEOL microscope – ref. JSM6490LV. Representative images were captured at 50X, 100X, and between 250 and 1000X.

Degradability assay

Degradability rates of produced scaffolds must be evaluated to determine if they match the rates at which new tissue is being produced, or to establish if they hinder this process (18, 19). To determine degradability rates, 25 to 60 mg of lyophilized native tissue and decellularized samples were immersed in 1X PBS (for 1L of 10X PBS: 26.83 mM KCl, 14.70 mM KH_2PO_4, 1.37 mM NaCl, 84.53 mM Na_2HPO_4, appropriate amount of 1N NaOH or 1N HCl to adjust pH to 7.4) or simulated body fluid buffer (SBF) (for 1L: 137.48 mM NaCl, 4.23 mM $NaHCO_3$, 3.02 mM KCl, 1.01 mM $K_2HPO_4 \cdot 3H_2O$, 1.53 mM $MgCl_2 \cdot 6H_2O$, 39 ml of 1M HCl, 2.63 mM $CaCl_2$, 506.89 µM Na_2SO_4, 50.51 mM Tris, 0-5ml of 1M to adjust pH to 7.4) at 37°C, to simulate physiological fluid conditions (20). This process was carried out for eight-weeks for PBS and six-weeks for SBF. After each week of immersion, samples were rinsed with distilled water, re-lyophilized and weighed to measure degradation, and the degradation rate was calculated based on the weekly percentage of sample mass loss compared

to initial weight, and the results obtained from PBS and SBF immersion were compared to determine an average degradability rate (20, 21). The average of weight loss was calculated from three replicates of each sample.

Mechanical characterization

Mechanical testing was performed to determine the scaffold´s mechanical behavior under determined conditions and stress. All tests were performed at Universidad de Antioquia's mechanical testing laboratory using a Shimadzu AGS 50KN universal testing machine – Trapezium X software. Samples were cut into specific dimensions to obtain three replicates for the native tissue and each optimized decellularization method. Uniaxial tension testing was performed in lyophilized samples cut into 100 mm x 25 mm fragments. The universal testing machine was set up at a rate of 4 mm/min. Each test piece was rehydrated for 1 min with 1X PBS, and assembled by positioning the sample longitudinally, leaving 50 mm between each clamp as shown in Figure 1a (22). Samples were exposed to uniaxial tension until breakage and the results were used to calculate deformation at break, tensile strength, elastic modulus and yield point.

For the suture strength test, samples were cut into 75 mm x 25 mm fragments. The universal testing machine was set up at a rate of 100 mm/min. Sample preparation was performed by passing a 5 mm suture thread from one end and rehydrating for 1 min with 1X PBS. The mounting was performed by clamping the suture thread while being held by the upper jaw of the universal machine, and the lower jaw clamped the end of the specimen directly as shown in Figure 1b (23). The distance between the suture point to the upper grip was 20 mm, and the distance from that suture point to the lower jaw was 50 mm. Stress was applied in the suture thread until breakage and properties such as maximum displacement and maximum tensile strength were calculated.

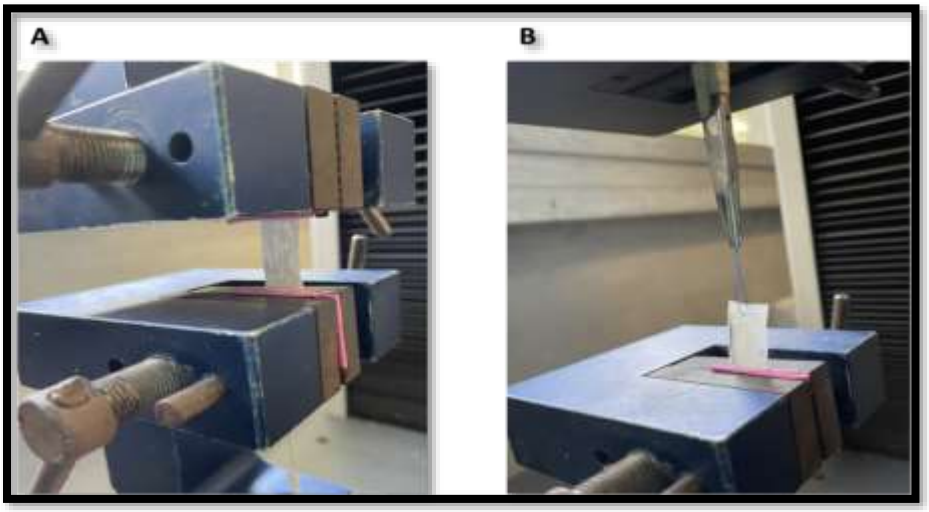

Figure 1. Mechanical testing of extracellular matrix-derived scaffolds. A. Uniaxial tension test for samples in universal testing machine. **B.** Suture strength test for samples in universal testing machine.

Statistical analysis

Statistical analyses for all data were performed using Jamovi (The jamovi project (2021). *Jamovi* (Version 1.6) [Computer Software]. Retrieved from https://www.jamovi.org). Results are shown as the mean ± standard deviation. For all measurements, one-way ANOVA or Kruskal-Wallis test was performed. A value of $p < 0.05$ was considered statistically significant.

RESULTS

Porcine small intestine decellularization

Initial qualitative analysis of decellularized porcine small intestine showed a gross color change throughout the tissue while maintaining the three-dimensional structure of all samples (Figure 2). Structural integrity was unchanged in most cases, except for Triton X-100 samples treated with two cycles of six and twenty-four hours, both of which showed augmented viscosity and structural weakening. Likewise, some samples exposed to two 24-hour cycles of SDS and SDC treatment showed a decrease on the tissue's density.

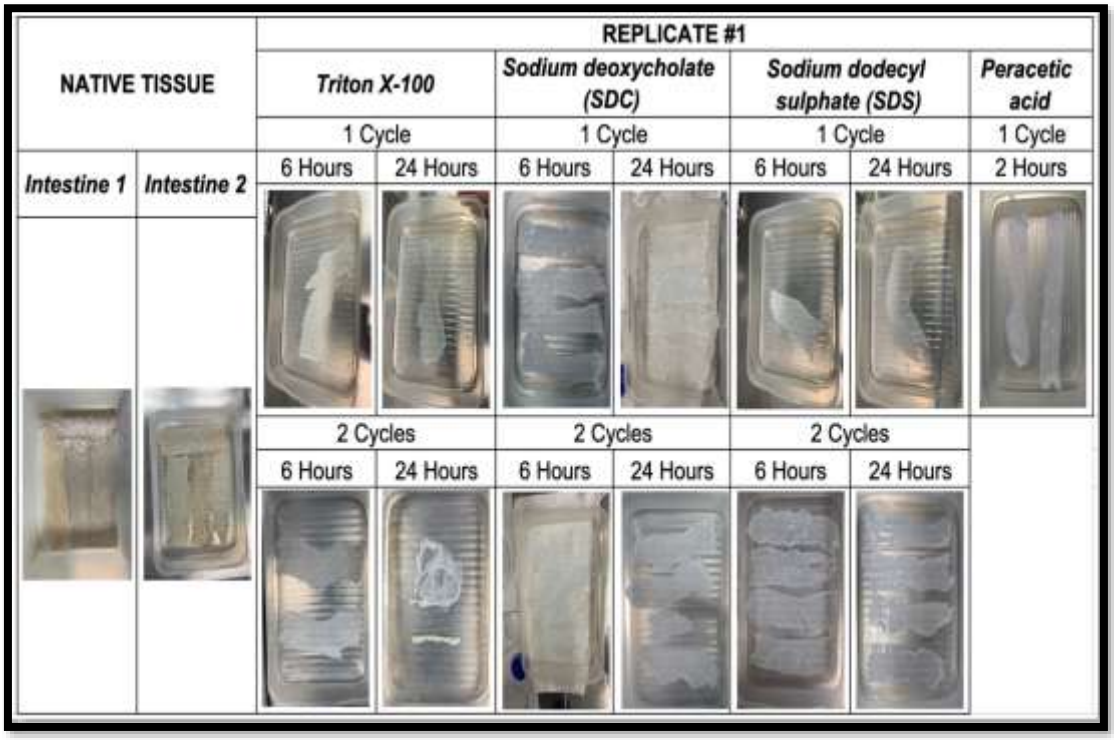

Figure 2. Representative images of porcine small intestine decellularization replicates, classified according to treatment agent, number of cycles, and time of exposure.

DNA quantification

DNA quantification of decellularized samples showed a reduced concentration for all treated specimens compared to native tissue (Figure 3A). The results indicated that an increase in time of exposition did not reduce the genetic content, as concentrations of nucleic acids for each sample in one six-hour cycle were similar to the same sample group (SDS, Triton X-100, or SDC) exposed for longer periods.

Particularly, for the decellularized scaffolds in one six-hour cycle, the concentrations of remnant DNA were: samples treated with peracetic acid showed the highest nucleic acid concentration out of the four treatment groups with an average of 10,752 ng/mg DNA compared to 15,374 ng/mg DNA in native tissue, showing a 30.06% decrease in nucleic acid concentration. Samples processed with Triton X-100 contained 2,889.5 ng/mg DNA, with a 77.72% decrease rate. On the other hand, samples decellularized with SDS presented a lower concentration at 754.25 ng/mg, with a 93.65% decrease rate. Finally, samples processed with SDC had the lowest concentrations at 466.25 ng/mg and a 96.60% decrease from native tissue concentrations.

The size of DNA fragments was observed through electrophoresis. Electrophoresis showed the absence of large nucleic acid fragments for all decellularized samples, with small fragments containing less than 1,000 nucleotides, present in most samples (Figure 3B). Peracetic acid samples showed a higher rate of degraded DNA in all replicates, furtherly validating the previous quantification results.

The nucleic acid concentrations and electrophoresis results were compared to determine the best method from the groups in comparison. Based on these results, the one six-hour cycle decellularization protocol was deemed as the best option to continue with subsequent characterizations for TX-100, SDS, and SDC specimens, while a one two-hour cycle was chosen for peracetic acid exposure.

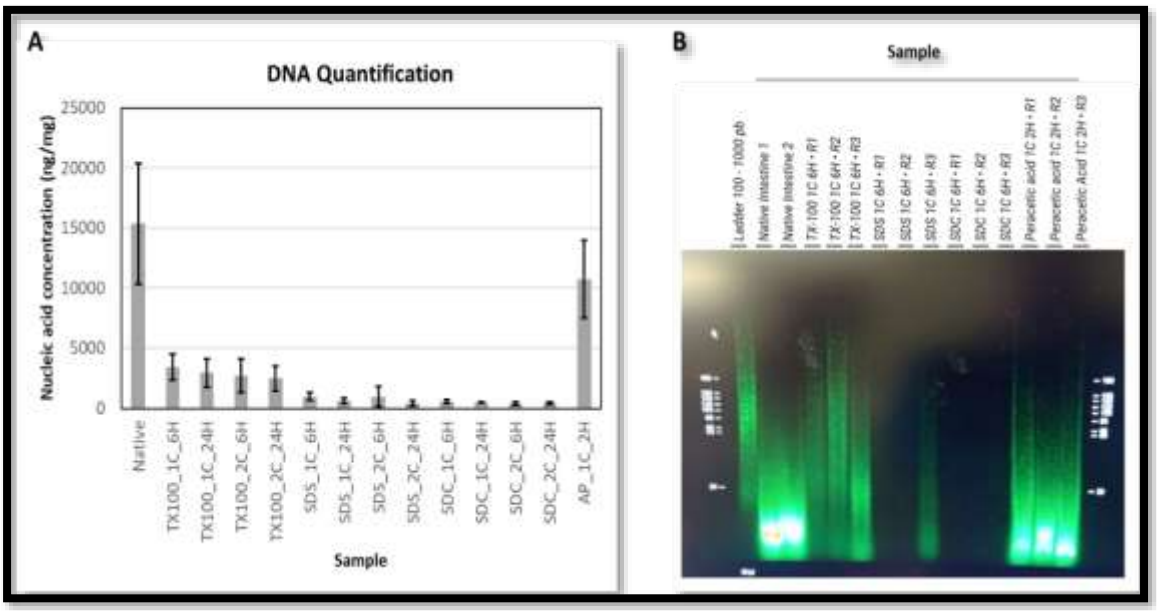

Figure 3. Quantification of DNA in remnant tissues. A. Average nucleic acid concentrations (ng) for native tissue and first three replicates of Triton X-100, SDS, SDC and peracetic acid per mg of sample. Decellularization groups are classified as follows: chemical agent used, cycles (C), and time of exposure per cycle (H). Bars represent the average of three replicates and the error bars represent the standard deviation. **B.** Electrophoresis of native tissue and first three replicates of one six-hour cycle treatments in 1% agarose gel for nucleic acid fragment visualization. Electrophoresis of native tissue and first three replicates in 1% agarose gel for nucleic acid fragment visualization. Samples are labeled according to number of cycles (C), exposure time (H) and replicate number (R).

Histological analysis

Hematoxylin and eosin staining was used to characterize the general structure of the tissue within the decellularized specimens in comparison with native tissue. Representative images were selected from the specimen sections of native tissue, TX-100, SDS, SDC, and peracetic acid. The native tissue control showed an organized low-density tissue with cell nuclei (Figure 4A) and well-defined external muscular layer and internal mucous layer. All specimens showed a significant drop in cellular content and have identifiable alterations to the tissue's integrity. Triton X-100 showed the most similarities to the native tissue, maintaining the muscular layer and fiber order throughout the tissue. Fiber count and proximity was slightly reduced, as well as the tubular structures' integrity in the mucous layer. SDS and SDC samples showed the most changes, significantly reducing the tissue density, fiber count and layer integrity. Peracetic acid specimens showed less severe alterations in the tissue's

integrity, fiber count and density, but still significant compared to native sections.

SEM was performed (Figure 4B) to obtain surface-level images of native tissue and the four optimized decellularized specimens. Native tissue surface imaging showed a highly organized and abundant count of collagen fibers both internally and externally throughout the tissue. The fiber networking was closely packed and unidirectionally positioned in the inner lining of the lumen, showing thick, plicated fibers as seen at 100X magnification. The external layer showed a more complex network of thinner fibers. Porosity was considered normal for the tissue, showing a high count of small pores. Biological remnants such as cell nuclei and adipose tissue were observed.
SEM of decellularized samples revealed similar results for TX-100 specimens, with a high count of organized collagen fibers, only slightly changing their positioning as showed at 100X magnification in the lumen; while its integrity was maintained, biological remnants were absent in these samples. Matrix porosity was not significantly affected, as it maintained similar qualitative results when compared with native tissue. Physical integrity was almost unaffected both internally and externally at surface level, indicating low alteration.

The SDS samples showed an important reduction on fiber count and thickness, loss of native porosity, and disorganization throughout the fibers: the lumen was significantly affected as observed at 100X magnification. SDC showed similar results with a lower reduction of fibers and thickness, and reduced porosity alterations. Peracetic acid treatment proved to be less abrasive while still reducing the amount of fiber and their density, however, some superficial biological remnants can still be identified.

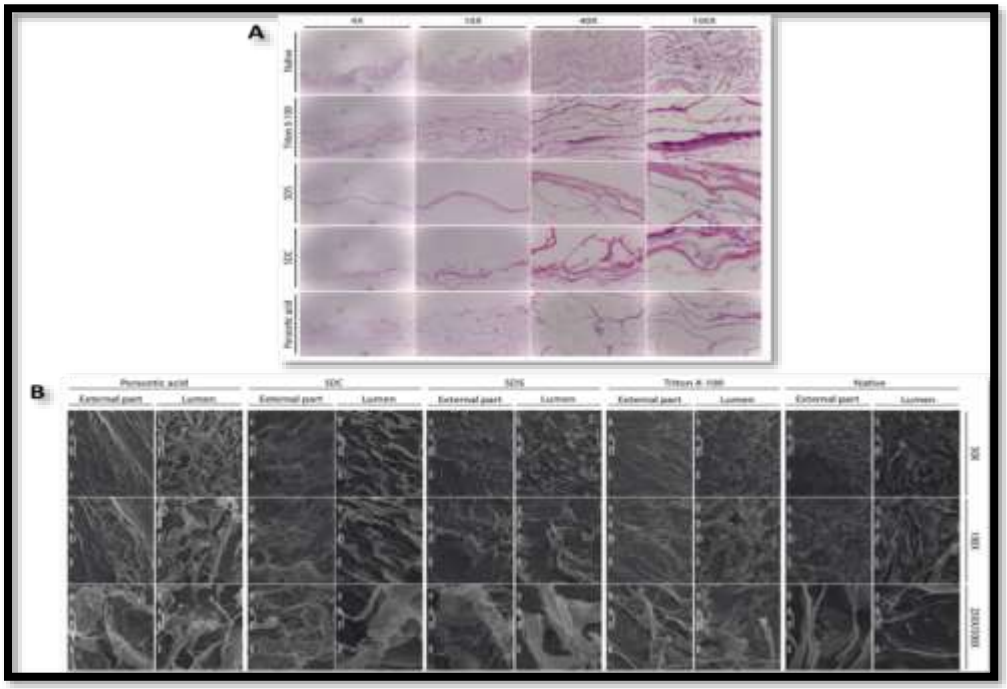

Figure 4. Scaffold structure after decellularization. A. Hematoxylin and eosin staining of native tissue and optimized decellularized specimens under compound microscope. Tissue morphology and integrity can be visualized for the native control tissue, Triton X-100, SDS, SDC and peracetic acid from top to bottom, with 4X, 10X, 40X, and 100X optical magnifications from left to right. **B.** Native tissue and optimized decellularized specimen imaging under scanning electron microscopy. Microstructure organization and matrix surface can be visualized for peracetic acid, SDC, SDS, Triton X-100 and native control tissue from left to right, with 50X, 100X, and 250/500X magnifications from top to bottom.

Degradability assay

Native tissue and decellularized lyophilized samples were cultured in PBS or SBF for eight and six-week total respectively, changing the solution each week to determine dry-weight changes due to matrix degradation. PBS was used for an initial degradability assay for all samples, and after protocol optimization based on nucleic acid quantification, a SBF degradability assay was implemented for samples treated under one six-hour cycle with TX-100, SDS, and SDC, and for one two-hour cycle with peracetic acid (Figure 5). Measurements were obtained and added to a week-to-week spreadsheet to quantify weight-loss and develop the degradability graphs.

After one week of PBS treatment the biggest decrease in mass was evidenced, having the highest degradation rate at 28.23% average mass loss from the original sample's measurements. The second week of treatment showed atypical results with a mass increase for all samples due to technical issues with the equipment, which will be analyzed in the discussion section. After the third week of treatment and onward, a steady decrease of total mass was recorded: degradation rates every week were around 5 and 21% of mass loss from the previous week, with some atypical values that will be discussed later. After eight weeks of treatment, mass loss surpassed 50% from original measurements for all samples.

On the other hand, after one week of SBF treatment only the samples treated with TX-100 and SDS experienced their biggest decrease in mass (35,57% on average) from the original measurements. But, for samples treated with SDC and Peracetic acid, as well as the native samples, the biggest decrease in mass was evidenced after two weeks of SBF immersion (42,05% on average) from the previous week. However, a steady decrease of total mass was recorded throughout the six-week immersion period: degradation rates every week were around 13% and 25% from the previous week. After the finalization of the treatment, mass loss surpassed 58% from original measurements for all samples.

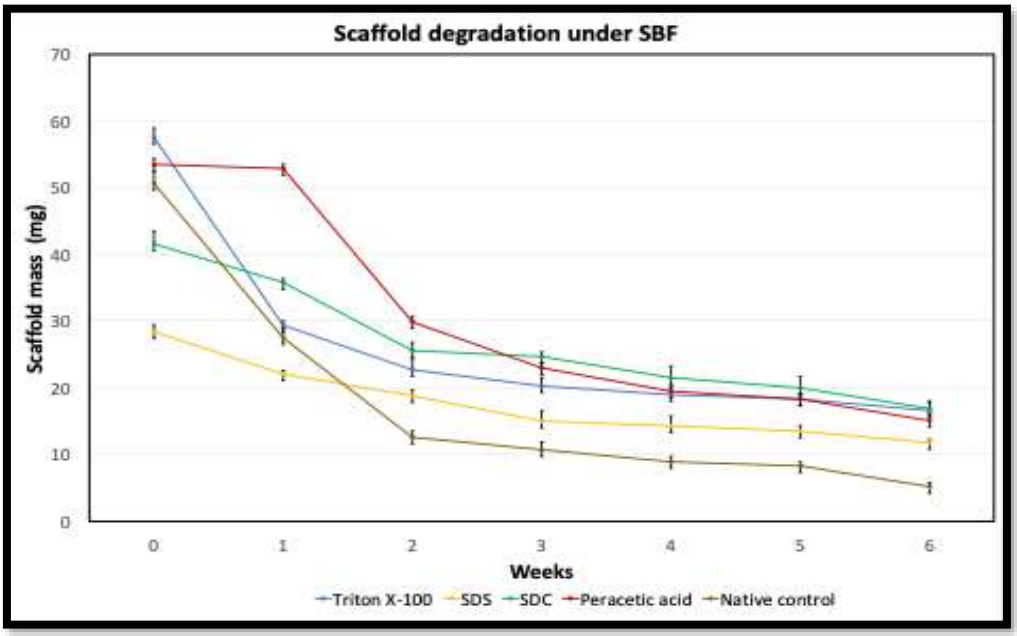

Figure 5. Degradation assay of extracellular matrix-derived scaffolds. Mass variation of native tissue and decellularized specimens in mg under SBF immersion for a six-week period, averaged by replica of each sample. Lines represent the average of three replicates and the error bars represent the standard deviation.

Mechanical characterization

Mechanical characterization was performed using a universal testing machine. The properties studied were determined under humid conditions for both the uniaxial tension test (Figure 6) and the suture strength test (Figure 7), in order to simulate the physiological conditions of the skin. Only the average of the data obtained by the universal machine was used and the deviation in respect of the mean was calculated, even if there were atypical data obtained.

The deformation at break points ranged from 0.290 ± 0.004 mm/mm to 0.595 ± 0.417 mm/mm (Figure 6A). No significant differences were reported among groups for deformation break point measurements (p=0.112). Tensile strength measurements were obtained, with values ranging from 3,29 ± 1.99 MPa to 6.68 ± 2.48 MPa, showing no statistical differences within the compared samples (p=0.500) (Figure 6B). Elastic modulus values were obtained, with the highest value at 23.50 ± 11.83 MPa and the lowest at 12.06 ± 5,.37 MPa (Figure 6C). Finally, yield point data ranged from 6.05 ± 2.48 MPa to 6.05 ± 2.48 MPa. For both the elastic modulus and yield point values, statistical differences were not determined within groups (p=0.129 and p=0.555, respectively) (Figure 6D).

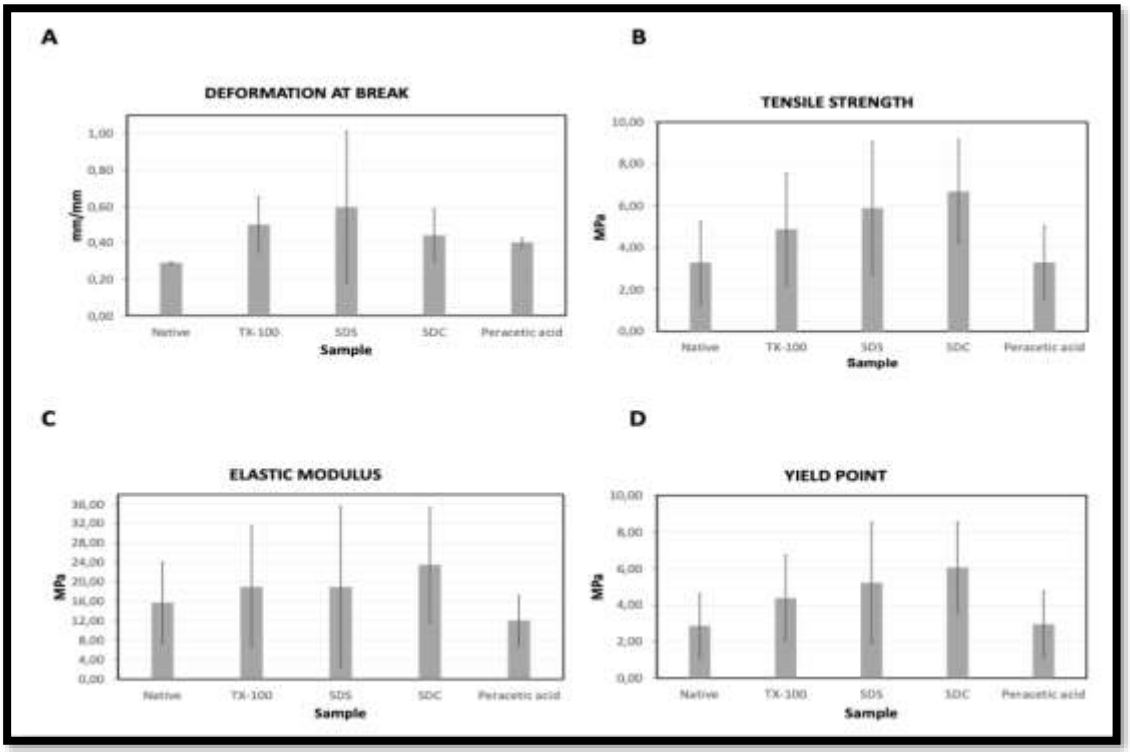

Figure 6. Uniaxial tensile test. A. Average results for deformation at break, **B**. tensile strength, **C**. elastic modulus, and **D**. yield point for all samples evaluated. Bars represent replicates average with error bars for standard deviation.

At the suture retention test, tensile strength evaluation showed peak values at the maximum displacement, providing a curve with a steep downward trend, which indicates that detachment occurred, and/or there was a rupture at the suture point.

The highest maximum displacement reached had a value of 14.87 ± 3.426 mm and the lowest of 8.78 ± 5.48 mm. No significant differences were found among groups for maximum displacement in this assay (p=0.257) (Figure 7A).

On the other hand, the maximum tensile strength ranged from 1.29 ± 0.22 N to 2.42 ± 0.82 N. There were no significant differences in the maximum tensile strength among groups in this assay (p=0.147) (Figure 7B).

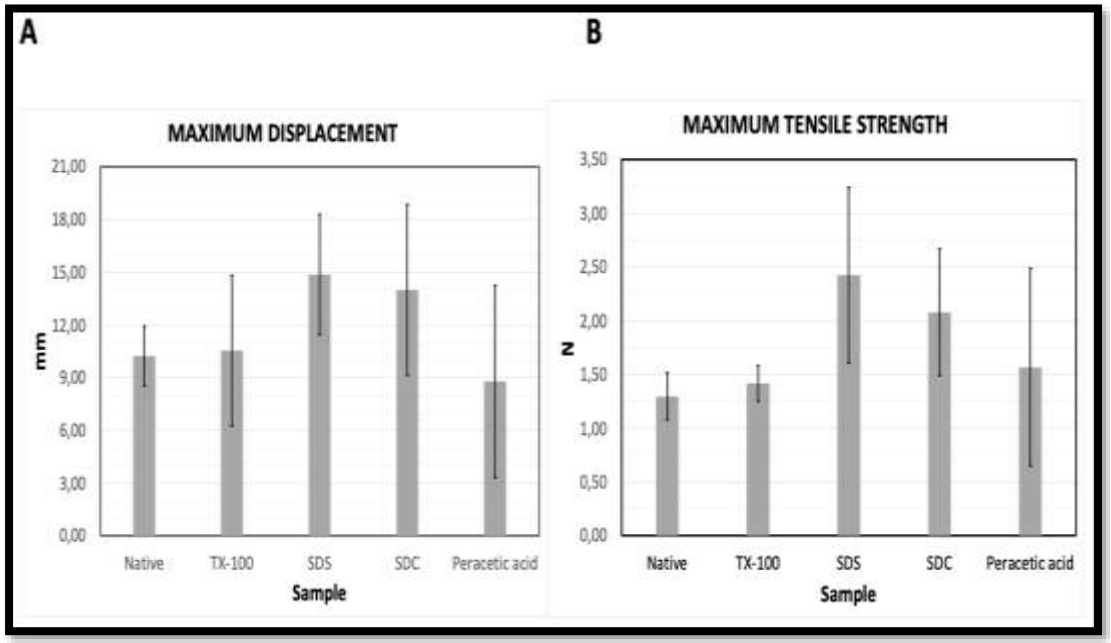

Figure 7. Suture retention assay. A. Average results for maximum displacement and tensile strength for all samples evaluated. Bars represent replicates average with error bars for standard deviation. **B.** Force/displacement curves for native and treated samples, each line representing a different replicate.

DISCUSSION

The skin is the largest organ in the human body and serves as an external cover to protect it from physical and biological agents such as heat and cold, humidity, sunlight, germs, bacteria, toxic or abrasive substances, among others (24). Beside protection, the skin provides thermal regulation, water and protein storage, mechanical sensitivity (25).

The skin can be affected by a series of conditions such as aging, physical damage, degenerative diseases, congenital defects, burns, among others (26-28). Any condition altering the integrity and stability of the skin results in dermal wounds (29). Dermal wounds reduce or affect the mechanical and protective properties of the tissue, increasing its susceptibility to diseases, and causing functional problems (30).

Wound healing is a complex biological mechanism that involves multiple interconnected biochemical signals to restore tissue integrity (31). Cutaneous wound healing is an essential physiological process that depends on multiple factors and cells, and includes four stages: hemostasis, inflammation, cell proliferation, and finally tissue remodeling (29). Multiple factors can affect wound healing, including the extent and depth of the damage, the progression stage of a preexisting condition, and the correct functioning of the immune system, resulting in drastic effects that reduce the quality of life and increase the patient morbidity and mortality (32, 33).

The extracellular matrix (ECM) is rich in structural and non-structural proteins that promote cellular growth and differentiation, tissue organization, and provide physical support and an ideal microenvironment for tissue repair (34, 35). It plays

a key role in cellular behavior given its biochemical cues that control and regulate cell function and disposition for organic growth and in injury response (36), improving and guiding tissue regeneration as previously reported (37-40). Furthermore, decellularized extracellular matrix has proven to be an effective alternative for skin tissue repair (41-44) by promoting cellular growth and improving reparative cues.

Multiple decellularization protocols were developed to certify the agent's efficacy and to determine which one is more efficient in genetic and cellular content removal while maintaining important functional cues and biocompatibility. Preliminary DNA quantification and electrophoresis results were considered for the optimal protocol selection. It is worth noting that different sections from the small intestine were used throughout the study, as no anatomical sectioning or exclusion criteria was performed for healthy pieces, hence some results may show variations between replicates.

Initial qualitative assessment of decellularized specimens established that all protocols result in the porcine tissue decellularization evidenced by the integral color changes: all samples lost its redness and adopt a transparent white coloring as cellular content and blood were removed and the extracellular matrix microstructure is preserved (45, 46). Most treated specimens showed no changes to their physical integrity in terms of texture, elasticity, density, and size. Samples exposed to Triton X-100 for extended periods suffered mechanical changes: all matrices treated for two 24 hour-cycles and one for two six hour-cycles presented higher viscosity, integral weakness, and some showing tears due to intrinsic changes to its strength and density. Similarly, specimens treated with SDS and SDC for two 24 hour-cycles showed reduced densities evidenced by an increased sheerness. This could be attributed to chemical overexposure, which can produce irreversible damage to the extracellular matrix's structural, biochemical, and mechanical properties (47), and, given the low-density of the small intestine, detergent treatment times must be limited to avoid tissue affection (48). Regarding SDS and SDC specimens, structural damage ensued given their high-charged ionic nature: more abrasive effects are expected when using ionic detergents (49) as they can produce high-levels of damage to ECM protein and structural components (50).

Nucleic acid concentrations were evaluated to determine quantitative decellularization efficacy. The results showed a drop in DNA concentration for TX-100, SDS, and SDC specimens, which is achieved thanks to cell membrane solubilization by chemical aqueous exposure which promotes cellular and genetic material removal (51). Peracetic acid decellularization has been explored in the past for tissue decellularization (52, 53), however, results showed non-effectiveness, which could be attributed to limited exposure times or the low concentration used (48). Given how TX-100, SDS, and SDC nucleic acid values were not different, decellularization affection on the biochemical, mechanical, and integral level should be considered further.

Throughout all the tests, electrophoresis showed low nucleic acid concentrations with small, degraded DNA fragments with low molecular weights for TX-100, SDS and SDC specimens. It is considered that fragmented DNA in electrophoresis gels with a less than 200 bp length does not present risk of immunoreactions (51), and residual, degraded DNA is not likely to be involved in adverse effects on tissue remodeling (54); deeming these matrices safe-to-use in a nucleic acid level; however, DAPI staining should be performed to comply with decellularization standards (51, 54). Peracetic acid did not show as favorable results as it does not satisfy the previously mentioned parameters: while residual

DNA is highly degraded, concentration values and length exceed safety limits.

Hematoxylin and Eosin staining was performed to evaluate tissue integrity, including collagen fiber count, orientation and organization, tissue density, and changes in inner and outer layers. All samples were visibly affected by decellularization, so the grade of damage must be evaluated. Triton X-100 histology showed a mostly preserved fiber organization and orientation, muscular external layer and mucous internal layer, and density, while showing affections to the tubular disposition of the mucous and a reduced fiber count, which can be attributed to the lengthy exposure time of unchanged solution (47). Some cells can be observed at 100X, however, decellularization promotes cell disruption which stops function and remove them from the tissue (55), and chemical detergents dissociate inner cell structure and contents (56) including the nuclei (51), supporting the idea that remnant cell content is non-functional and will not induce immune reactions. However, this must be verified by DAPI staining to assure application safety. SDS and SDC histology showed a reduction in density, tissue organization, fiber count, and differentiation between layers, affecting ECM integrity throughout the tissue. Effects can be ascribed to detergent strength as ionic detergents are abrasive in non-optimal applications (47). Some cells can be observed at 100X on SDC samples, and by concepts described previously it is believed that they do not present a rejection risk, especially given their size. Peracetic acid samples show significant differences between native and treated samples, but they are less severe when reviewing fiber qualities and tissue density, which is due to the subdued chemical strength (57). Imaging analysis should be performed to further understand the obtained data and quantify the observed changes.

Extracellular matrix porosity, topography, and organization was analyzed through high-quality SEM imaging to accompany histological evaluation. Treated samples showed changes to the matrix at a surface level, which are attributed to the chemical treatments used in this study (47). Triton X-100 showed the least drastic changes in the extracellular matrix at a surface level, maintaining an organized and abundant fibrous structure that resembles that observed in the native tissue, while only slightly increasing porosity. Non-ionic detergents are less abrasive and more effective at maintaining biochemical and mechanical cues on low-density tissues (58), which is crucial for effective regenerative skin applications. Moreover, preserving porosity is crucial for the reparative potential as it is needed to allow for a controlled diffusion of biochemical cues from the ECM associated to skin repair (59).

SDS and SDC showed higher affections to the matrix surface, with a loss of fiber thickness and changes to the organization and porosity being a concern. This is due to the strength of both detergents and how integrity can be disrupted as previously mentioned. Peracetic acid samples showed less drastic effects, however, a concern in immunogenicity is raised given the superficial biological remnants identified, which could increase the risk of rejection and other complications in a clinical setting (60). Further analysis of these images must be performed to confirm or change the views obtained in the qualitative analysis performed.

Degradability assays were performed to determine dry weight changes due to matrix degradation using PBS and SBF buffers. Results show that both buffers produced loss of total mass in all samples, as expected since both of them simulate some of the body fluid natural characteristics, and matrix derived from biological sources are degradable (61). However, there were some differences between the results obtained from both assays. The degradation assay with PBS, showed a general lower final percentage loss from all samples than

SBF, as well as a much slower degradation rate across the immersion period. These differences can be explained with the variances in the chemical composition of each buffer, with SBF having a more complete and more similar composition to that of blood plasma (21). Therefore, degradation under SBF can be expected to be faster than PBS and to more accurately describe that which is seen under normal body conditions, as observed in this study.

As previously mentioned, atypical results were observed throughout the degradability assays that can be explained due to equipment performance issues and matrix composition. Issues regarding recalibration of the analytical balances used for the weight loss studies affected some of the measurements, especially those in the PBS protocol which in result could have affected the analysis of weight loss percentage. Furthermore, all samples were lyophilized again after each week of immersion to ensure complete dryness. However, this process depends on the complete freezing of samples, which can be affected due to considerable concentrations of alcohols and/or detergents present in the samples (62, 63). All the mentioned components could be considered present in the processed samples in this study, due to its tissue of origin and the processing itself. Therefore, measurements of total weight loss and between weeks could have been affected by the constant lyophilization of the samples, possibly explaining some of the atypical values.

Both degradability assays could be used to describe the obtained matrix regarding their possible performance in a clinical setting. Degradation times point to a possible regeneration potential without mass loss of the matrix degradable properties or clinical complications such as fibrotic encapsulation, which is not desired since it can prevent normal tissue regeneration (64). The present study demonstrated an approximated 60% loss of total mass on all samples, which can be compared to the degradability percentage observed in graft application of similar matrices (65, 66). Further studies that explore morphological and molecular changes should be performed to retrieve more data as done in previous studies (21).

In vivo the submucosa of the small intestine is subjected to multidimensional stresses (67), so mechanical stress tests were performed to obtain an estimation of the behavior. No significant differences were found in the effects of each method on the mechanical properties. However, it has been shown that some acids, when used in ECM, can alter its mechanical properties (52), which explains the reason for the affected structure of the peracetic acid-treated matrices, meaning that they might be less flexible than the matrices obtained by the other methods (52). It was expected that after treatment with detergents for decellularization, when comparing the matrices resulting from each method with the native tissue in the mechanical studies, no changes in the structure would be reflected, which could be confirmed with the results obtained and the non-significancy in their differences.

The bars shown in the graphs for the properties of the matrices treated with SDS, TX-100 and SDC showed high values for the evaluated criteria. However, it has been previously described that the use of detergents can be harmful to ECM (68), which was not evidenced in this study since there is no significant differences within the treatments and the native tissue. Now, the difference in properties of the replicas may be due to the origin, its age (69) and the fragment taken from the intestine, which were not discriminated in this study. This is evident in the variability between the uniaxial tensile and suture strength data and is attributed to the anisotropy present in the ECM due to the fibrillar distribution within the matrix (52).

All preliminary evaluations and subsequent histology analysis point to the one six-hour cycle of Triton X-100 immersion protocol to be the most

efficient given the results of DNA concentration and size, and tissue integrity. Its mild method of action is ideal for low density tissues like the small intestine (51, 70) including small intestine (40, 69, 71), making it less likely for the ECM to suffer from severe disruptions to its structure and biochemical composition. Further characterization must be performed to determine whether this would be the case, especially since this protocol did not yield relatively good results in the mechanical assays. Additionally, larger sample sizes should be considered so stronger statistical analysis may be performed.

AUTHORS' CONTRIBUTIONS: All the authors participated in: conception and design of the study, data collection, analysis and interpretation, drafting of the article, critical review and approval of the final version, and are responsible for the veracity and integrity of the article.

CONFLICTS OF INTEREST: the authors declare no conflicts of interest for the conduct and publication of this case report.

FUNDING: This work was supported by the Colombian Ministry of Science, Technology, and Innovation (Minciencias) Contract 425 of 2021 (Jóvenes Talento) and Universidad CES.

REFERENCES

1. Karimkhani C, Dellavalle RP, Coffeng LE, Flohr C, Hay RJ, Langan SM, et al. Global Skin Disease Morbidity and Mortality: An Update From the Global Burden of Disease Study 2013. JAMA Dermatology. 2017 May 1;153(5):406–12.

2. Hay RJ, Johns NE, Williams HC, Bolliger IW, Dellavalle RP, Margolis DJ, et al. The Global Burden of Skin Disease in 2010: An Analysis of the Prevalence and Impact of Skin Conditions. Journal of Investigative Dermatology. 2014 Jun 1;134(6):1527–34.

3. Lo ZJ, Lim X, Eng D, Car J, Hong Q, Yong E, et al. Clinical and economic burden of wound care in the tropics: a 5-year institutional population health review. International Wound Journal. 2020;17(3):790–803.

4. World Health Organization, editor. The injury chart book: a graphical overview of the global burden of injuries. Geneva: Dept. of Injuries and Violence Prevention, Noncommunicable Diseases and Mental Health Cluster, World Health Organization; 2002. 75 p.

5. González Consuegra RV, Roa Lizcano KT, López Zuluaga WJ. Estudio de prevalencia de lesiones por presión en un Hospital Universitario, Bogotá-Colombia. Rev cienc cuidad. 2018 Jun 30;15(2):91–100.

6. Rowan MP, Cancio LC, Elster EA, Burmeister DM, Rose LF, Natesan S, et al. Burn wound healing and treatment: review and advancements. Crit Care [Internet]. 2015 [cited 2021 Jun 11];19. Available from: https://www.ncbi.nlm.nih.gov/pmc/articles/PMC4464872/

7. Salamone JC, Salamone AB, Swindle-Reilly K, Leung KXC, McMahon RE. Grand challenge in Biomaterials-wound healing. Regenerative Biomaterials. 2016 Jun 1;3(2):127–8.

8. Sarkar K, Xue Y, Sant S. Host Response to Synthetic Versus Natural Biomaterials. In: Corradetti B, editor. The Immune Response to Implanted Materials and Devices: The Impact of the Immune System on the Success of an Implant [Internet]. Cham: Springer International Publishing; 2017 [cited 2021 Jun 11]. p. 81–105. Available from: https://doi.org/10.1007/978-3-319-45433-7_5

9. Su Y, Zhang X, Ren G, Zhang Z, Liang Y, Wu S, et al. In situ implantable three-dimensional extracellular matrix bioactive composite scaffold for postoperative skin cancer therapy. Chemical Engineering Journal. 2020 Nov 15;400:125949.

10. Parmaksiz M, Dogan A, Odabas S, Elçin AE, Elçin YM. Clinical applications of decellularized extracellular matrices for tissue engineering and regenerative medicine. Biomed Mater. 2016 Mar;11(2):022003.

11. Tajima K, Kuroda K, Otaka Y, Kinoshita R, Kita M, Oyamada T, et al. Decellularization of canine kidney for three-dimensional organ regeneration. Vet World. 2020 Mar;13(3):452–7.

12. Oliveira AC, Garzón I, Ionescu AM, Carriel V, Cardona J de la C, González-Andrades M, et al. Evaluation of

Small Intestine Grafts Decellularization Methods for Corneal Tissue Engineering. PLOS ONE. 2013 Jun 14;8(6):e66538.

13. Maghsoudlou P, Totonelli G, Loukogeorgakis SP, Eaton S, De Coppi P. A Decellularization Methodology for the Production of a Natural Acellular Intestinal Matrix. J Vis Exp. 2013 Oct 7;(80):50658.

14. Keane TJ, Londono R, Turner NJ, Badylak SF. Consequences of ineffective decellularization of biologic scaffolds on the host response. Biomaterials. 2012 Feb;33(6):1771–81.

15. Gilbert TW, Freund JM, Badylak SF. Quantification of DNA in biologic scaffold materials. J Surg Res. 2009 Mar;152(1):135–9.

16. Lee PY, Costumbrado J, Hsu CY, Kim YH. Agarose Gel Electrophoresis for the Separation of DNA Fragments. J Vis Exp. 2012 Apr 20;(62):3923.

17. Freytes DO, Martin J, Velankar SS, Lee AS, Badylak SF. Preparation and rheological characterization of a gel form of the porcine urinary bladder matrix. Biomaterials. 2008 Apr;29(11):1630–7.

18. Control of Scaffold Degradation in Tissue Engineering: A Review | Tissue Engineering Part B: Reviews [Internet]. [cited 2022 Aug 26]. Available from: https://www.liebertpub.com/doi/10.1089/ten.teb.2013.0452

19. Park SH, Gil ES, Shi H, Kim HJ, Lee K, Kaplan DL. Relationships Between Degradability of Silk Scaffolds and Osteogenesis. Biomaterials. 2010 Aug;31(24):6162–72.

20. Sasikumar Y, Solomon MM, Olasunkanmi LO, Ebenso EE. Effect of surface treatment on the bioactivity and electrochemical behavior of magnesium alloys in simulated body fluid: Effect of surface treatment on the bioactivity. Materials and Corrosion. 2017 Jul;68(7):776–90.

21. Barbeck M, Serra T, Booms P, Stojanovic S, Najman S, Engel E, et al. Analysis of the in vitro degradation and the in vivo tissue response to bi-layered 3D-printed scaffolds combining PLA and biphasic PLA/bioglass components – Guidance of the inflammatory response as basis for osteochondral regeneration. Bioact Mater. 2017 Jun 23;2(4):208–23.

22. Zhao S, Gu L, Hammel JM, Lang H. Mechanical Characterization of the Decellularized Porcine Small Intestinal Submucosa Extracellular Matrix. In: Volume 3A: Biomedical and Biotechnology Engineering [Internet]. San Diego, California, USA: American Society of Mechanical Engineers; 2013 [cited 2021 Dec 14]. p. V03AT03A082. Available from: https://asmedigitalcollection.asme.org/IMECE/proceedings/IMECE2013/56215/San%20Diego,%20California,%20USA/261133

23. Dearth CL, Keane TJ, Carruthers CA, Reing JE, Huleihel L, Ranallo CA, et al. The effect of terminal sterilization on the material properties and in vivo remodeling of a porcine dermal biologic scaffold. Acta Biomaterialia. 2016 Mar;33:78–87.

24. Dąbrowska AK, Spano F, Derler S, Adlhart C, Spencer ND, Rossi RM. The relationship between skin function, barrier properties, and body-dependent factors. Skin Res Technol. 2018 May;24(2):165–74.

25. Information NC for B, Pike USNL of M 8600 R, MD B, Usa 20894. How does skin work? [Internet]. InformedHealth.org [Internet]. Institute for Quality and Efficiency in Health Care (IQWiG); 2019 [cited 2021 Jun 11]. Available from: https://www.ncbi.nlm.nih.gov/books/NBK279255/

26. Khavkin J, Ellis DAF. Aging skin: histology, physiology, and pathology. Facial Plast Surg Clin North Am. 2011 May;19(2):229–34.

27. Rayner R, Carville K, Leslie G, Roberts P. A review of patient and skin characteristics associated with skin tears. J Wound Care. 2015 Sep;24(9):406–14.

28. Lazarus GS, Cooper DM, Knighton DR, Margolis DJ, Pecoraro RE, Rodeheaver G, et al. Definitions and guidelines for assessment of wounds and evaluation of healing. Arch Dermatol. 1994 Apr;130(4):489–93.

29. Singh S, Young A, McNaught CE. The physiology of wound healing. Surgery (Oxford). 2017 Sep 1;35(9):473–7.

30. Duscher D, Barrera J, Wong VW, Maan ZN, Whittam AJ, Januszyk M, et al. Stem Cells in Wound Healing: The Future of Regenerative Medicine? A Mini-Review. GER. 2016;62(2):216–25.

31. Gonzalez AC de O, Costa TF, Andrade Z de A, Medrado ARAP. Wound healing - A literature review*. An Bras Dermatol. 2016 Oct;91:614–20.

32. Guo S, DiPietro LA. Factors Affecting Wound Healing. J Dent Res. 2010 Mar;89(3):219–29.

33. Wernick B, Nahirniak P, Stawicki SP. Impaired Wound Healing. In: StatPearls [Internet]. Treasure Island (FL): StatPearls Publishing; 2022 [cited 2022 Aug 26]. Available from: http://www.ncbi.nlm.nih.gov/books/NBK482254/

34. Ha DH, Chae S, Lee JY, Kim JY, Yoon J, Sen T, et al. Therapeutic effect of decellularized extracellular matrix-based hydrogel for radiation esophagitis by 3D printed esophageal stent. Biomaterials. 2021 Jan 1;266:120477.

35. Wang S, Zhu C, Zhang B, Hu J, Xu J, Xue C, et al. BMSC-derived extracellular matrix better optimizes the microenvironment to support nerve regeneration. Biomaterials. 2022 Jan 1;280:121251.

36. Hussey GS, Dziki JL, Badylak SF. Extracellular matrix-based materials for regenerative medicine. Nat Rev Mater. 2018 Jul;3(7):159–73.

37. Ventura RD, Padalhin AR, Park CM, Lee BT. Enhanced decellularization technique of porcine dermal ECM for tissue engineering applications. Materials Science and Engineering: C. 2019 Nov 1;104:109841.

38. Lee SJ, Lee JH, Park J, Kim WD, Park SA. Fabrication of 3D Printing Scaffold with Porcine Skin Decellularized Bio-Ink for Soft Tissue Engineering. Materials. 2020 Jan;13(16):3522.

39. Kim BS, Kwon YW, Kong JS, Park GT, Gao G, Han W, et al. 3D cell printing of in vitro stabilized skin model and in vivo pre-vascularized skin patch using tissue-specific extracellular matrix bioink: A step towards advanced skin tissue engineering. Biomaterials. 2018 Jun 1;168:38–53.

40. Hussey GS, Dziki JL, Badylak SF. Extracellular matrix-based materials for regenerative medicine. Nat Rev Mater. 2018 Jul;3(7):159–73.

41. Xu J, Fang H, Zheng S, Li L, Jiao Z, Wang H, et al. A biological functional hybrid scaffold based on decellularized extracellular matrix/gelatin/chitosan with high biocompatibility and antibacterial activity for skin tissue engineering. International Journal of Biological Macromolecules. 2021 Sep 30;187:840–9.

42. Sarmin AM, El Moussaid N, Suntornnond R, Tyler EJ, Kim YH, Di Cio S, et al. Multi-Scale Analysis of the Composition, Structure, and Function of Decellularized Extracellular Matrix for Human Skin and Wound Healing Models. Biomolecules. 2022 Jun;12(6):837.

43. Liu Y, Huang CC, Wang Y, Xu J, Wang G, Bai X. Biological evaluations of decellularized extracellular matrix collagen microparticles prepared based on plant enzymes and aqueous two-phase method. Regenerative Biomaterials. 2021 Mar 1;8(2):rbab002.

44. Chou PR, Lin YN, Wu SH, Lin SD, Srinivasan P, Hsieh DJ, et al. Supercritical Carbon Dioxide-decellularized Porcine Acellular Dermal Matrix combined with Autologous Adipose-derived Stem Cells: Its Role in Accelerated Diabetic Wound Healing. Int J Med Sci. 2020 Feb 4;17(3):354–67.

45. Gratzer PF. Decellularized Extracellular Matrix. In: Narayan R, editor. Encyclopedia of Biomedical Engineering [Internet]. Oxford: Elsevier; 2019 [cited 2022 Jul 12]. p. 86–96. Available from: https://www.sciencedirect.com/science/article/pii/B9780128012383998702

46. Kim YS, Majid M, Melchiorri AJ, Mikos AG. Applications of decellularized extracellular matrix in bone and cartilage tissue engineering. Bioeng Transl Med. 2018 Oct 26;4(1):83–95.

47. Tan YH, Helms HR, Nakayama KH. Decellularization Strategies for Regenerating Cardiac and Skeletal Muscle Tissues. Frontiers in Bioengineering and Biotechnology [Internet]. 2022 [cited 2022 Jul 21];10. Available from: https://www.frontiersin.org/articles/10.3389/fbioe.2022.831300

48. Hrebikova H, Diaz D, Mokry J. Chemical decellularization: a promising approach for preparation of extracellular matrix. Biomedical Papers. 2015 Mar 9;159(1):012–7.

49. G-Biosciences. Detergents for Protein Extraction & Cell Lysis Guide [Internet]. 1st ed. United States; 2010 [cited 2021 May 9]. (1; vol. Protein Research). Available from: http://www.genotech.com/protein-research/detergent-accessories.html#:~:text=Detergents%20%7C%20Order%20Online-,ionic%20detergents,for%20separation%20during%20gel%20electrophoresis.

50. Zahmati AHA, Alipoor R, Shahmirzadi AR, Khori V, Abolhasani MM. Chemical Decellularization Methods and Its Effects on Extracellular Matrix. Internal Medicine and Medical Investigation Journal. 2017 Aug 4;2(3):76–83.

51. Gilpin A, Yang Y. Decellularization Strategies for Regenerative Medicine: From Processing Techniques to Applications. Biomed Res Int. 2017;2017:9831534.

52. Syed O, Walters NJ, Day RM, Kim HW, Knowles JC. Evaluation of decellularization protocols for production of tubular small intestine submucosa scaffolds for use in oesophageal tissue engineering. Acta Biomaterialia. 2014 Dec 1;10(12):5043–54.

53. Yamanaka H, Morimoto N, Yamaoka T. Decellularization of submillimeter-diameter vascular scaffolds using peracetic acid. J Artif Organs. 2020 Jun;23(2):156–62.

54. Wei F, Liu S, Chen M, Tian G, Zha K, Yang Z, et al. Host Response to Biomaterials for Cartilage Tissue Engineering: Key to Remodeling. Frontiers in Bioengineering and Biotechnology [Internet]. 2021 [cited 2022 Jul 21];9. Available from: https://www.frontiersin.org/articles/10.3389/fbioe.2021.664592

55. Fernández-Pérez J, Ahearne M. The impact of decellularization methods on extracellular matrix derived hydrogels. Sci Rep. 2019 Oct 17;9(1):14933.

56. Mendibil U, Ruiz-Hernandez R, Retegi-Carrion S, Garcia-Urquia N, Olalde-Graells B, Abarrategi A. Tissue-Specific Decellularization Methods: Rationale and Strategies to Achieve Regenerative Compounds. Int J Mol Sci. 2020 Jul 30;21(15):5447.

57. Tao M, Ao T, Mao X, Yan X, Javed R, Hou W, et al. Sterilization and disinfection methods for decellularized matrix materials: Review, consideration and proposal. Bioact Mater. 2021 Feb 27;6(9):2927–45.

58. White LJ, Taylor AJ, Faulk DM, Keane TJ, Saldin LT, Reing JE, et al. The impact of detergents on the tissue decellularization process: a ToF-SIMS study. Acta Biomater. 2017 Mar 1;50:207–19.

59. Moffat D, Ye K, Jin S. Decellularization for the retention of tissue niches. J Tissue Eng. 2022 May 21;13:20417314221101150.

60. Benichou G, Yamada Y, Yun SH, Lin C, Fray M, Tocco G. Immune recognition and rejection of allogeneic skin grafts. Immunotherapy. 2011 Jun;3(6):757–70.

61. Gilbert TW, Stewart-Akers AM, Badylak SF. A quantitative method for evaluating the degradation of biologic scaffold materials. Biomaterials. 2007 Jan 1;28(2):147–50.

62. Kasper JC, Friess W. The freezing step in lyophilization: Physico-chemical fundamentals, freezing methods and consequences on process performance and quality attributes of biopharmaceuticals. European Journal of Pharmaceutics and Biopharmaceutics. 2011 Jun 1;78(2):248–63.

63. Zagorska J, Ciprovica I. Evaluation of Factors Affecting Freezing Point of Milk. 2013;7(2):6.

64. Keane TJ, Dziki J, Castelton A, Faulk DM, Messerschmidt V, Londono R, et al. Preparation and characterization of a biologic scaffold and hydrogel derived from colonic mucosa. J Biomed Mater Res B Appl Biomater. 2017 Feb;105(2):291–306.

65. Gilbert TW, Stewart-Akers AM, Simmons-Byrd A, Badylak SF. Degradation and Remodeling of Small Intestinal Submucosa in Canine Achilles Tendon Repair. JBJS. 2007 Mar;89(3):621–30.

66. Record RD, Hillegonds D, Simmons C, Tullius R, Rickey FA, Elmore D, et al. In vivo degradation of 14C-labeled small intestinal submucosa (SIS) when used for urinary bladder repair. Biomaterials. 2001 Oct 1;22(19):2653–9.

67. Shi L, Ronfard V. Biochemical and biomechanical characterization of porcine small intestinal submucosa (SIS): a mini review. Int J Burns Trauma. 2013 Nov 1;3(4):173–9.

68. Crapo PM, Gilbert TW, Badylak SF. An overview of tissue and whole organ decellularization processes. Biomaterials. 2011 Apr 1;32(12):3233–43.

69. Singh H, Purohit SD, Bhaskar R, Yadav I, Gupta MK, Mishra NC. Development of decellularization protocol for caprine small intestine submucosa as a biomaterial. Biomaterials and Biosystems. 2022 Mar 1;5:100035.

70. Vavken P, Joshi S, Murray MM. TRITON-X Is Most Effective among Three Decellularization Agents for ACL Tissue Engineering. J Orthop Res. 2009 Dec;27(12):1612–8.

71. Faulk DM, Carruthers CA, Warner HJ, Kramer CR, Reing JE, Zhang L, et al. The Effect of Detergents on the Basement Membrane Complex of a Biologic Scaffold Material. Acta Biomater. 2014 Jan;10(1):10.1016/j.actbio.2013.09.006.